A Numerical Study of the Performance of a Heat Exchanger for a Miniature Joule-Thomson Refrigerator

Yong-Ju Hong[1], Seong-Je Park[1], and Young-Don Choi[2]

[1]Korea Institute of Machinery & Materials, Daejeon, Korea
[2]Department of Mechanical Engineering, Korea University, Seoul, Korea

ABSTRACT

Miniature Joule-Thomson refrigerators have been widely used for rapid cooling of infrared detectors, cryosurgery probes, thermal cameras, and missile guidance homing systems, due to their special features of simple configuration, compact structure and rapid cooldown characteristics. The thermodynamic performance of the J-T refrigerator depends upon the hydraulic and heat transfer characteristics of the recuperative heat exchanger. The typical recuperative heat exchanger of the J-T refrigerator has the double helical tube and fin configuration.

In this study, an effectiveness-NTU approach is adopted to predict the thermodynamic behaviors of the heat exchanger for the Joule-Thomson refrigerator. The thermodynamic properties from the NIST REFPROP[1] database is used to account for the real gas effects. The results show the effect of the operating conditions on the performance of the heat exchanger and refrigerator for the given heat exchanger. The influences of mass flow rate and the supply pressure on the effectiveness of heat exchanger and the ideal cooling capacity are discussed in details.

INTRODUCTION

Miniature Joule-Thomson (J-T) refrigerators have been widely used for rapid cooling of infrared detectors, cryosurgery probes, thermal cameras, and missile guidance homing systems, due to their special features of simple configuration, compact structure and rapid cooldown characteristics. Nitrogen (NBP 77.35 K) and argon gas (NBP 87.3 K) are typically used as the cryogen due to their availability, low cost and relatively low cryogenic temperature.

The cooldown time, the cold end temperature, the running time and the gas consumption are the important indicators of the Joule-Thomson refrigerator performance.

The cooling power of the J-T refrigerator is generated by the isenthalpic expansion of the high pressure gas through the throttling process. The J-T effect could be amplified by using an expanded gas to cool incoming gas within a recuperative heat exchanger. The thermodynamic performance of J-T refrigerator is highly dependent upon the hydraulic and heat transfer characteristics of the recuperative heat exchanger. The typical recuperative heat exchanger of the J-T refrigerator has the double helical tube and fin configuration to increase heat transfer area as shown in Figure 1.

Limited experimental and theoretical studies on the performance of the refrigerator were performed due to the complexity of the geometry of the recuperative heat exchanger of the

Cryocoolers 15, edited by S.D. Miller and R.G. Ross, Jr.

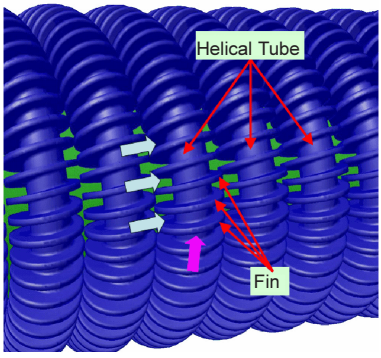

Figure 1. The typical recuperative heat exchanger of J-T refrigerator.

Joule-Thomson refrigerator. Ng et al.[2] and Xue et al.[3] reported the experimental and numerical study of the J-T refrigerator for steady-state characteristics with the argon gas. Numerical studies of J-T refrigerator with the nitrogen gas for transient characteristics with one dimensional transient model were reported by Chien et al.[4], Chou et al.[5], and Chua et al.[6] developed the geometry model of the Hampson-type cryocooler with argon gas as a cryogen. The steady state governing equations were solved numerically.

In this study, an effectiveness-NTU approach is adopted to predict the thermodynamic behaviors of the heat exchanger for the J-T refrigerator with nitrogen and argon gas.

RECUPERATIVE HEAT EXCHANGER

A schematic diagram of a J-T cooling cycle is found in Figure 2. It consists of a counter flow heat exchanger with helical fins, a pressure vessel, an evaporator (expansion space) and a J-T valve. From point 1 to point 2, the high pressure gas is cooled in the counter flow heat exchanger by the low pressure returning gas after J-T expansion (from point 2 to point 3).

An energy balance of the J-T valve requires that the specific enthalpy at the valve outlet must equal the specific enthalpy at the valve inlet.

$$h_3 = h_2 \tag{1}$$

The ideal cooling capacity at the evaporator is given by

$$Q_{ideal} = \dot{m}\,(h_4 - h_3) \tag{2}$$

where $\dot{m}$ is the mass flow rate.

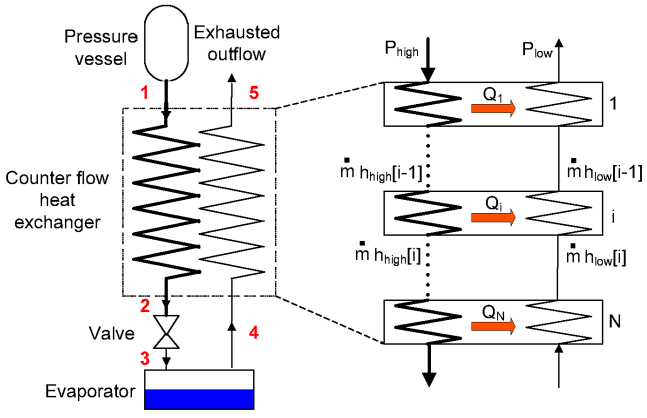

Figure 2. The schematic diagram of a J-T cooling cycle.

The enthalpy of high pressure gas leaving each element and the enthalpy of low pressure gas entering each element could be calculated according to

$$h_{high}\,[i] = h_{high}\,[i-1] - \frac{Q_i}{\dot{m}} \tag{3}$$

$$h_{low}\,[i] = h_{low}\,[i-1] - \frac{Q_i}{\dot{m}} \tag{4}$$

where Q_i is the recuperative heat transfer of each element. The heat transfer between the fluids is related to the temperature difference according to:

$$Q_i = \varepsilon C_{min}\,(T_{high}[i-1] - T_{low}[i]) \tag{5}$$

where ε is the effectiveness of each element and C_{min} is smaller capacity rate between two recuperating stream.

The effectiveness-NTU relationship associated with a counter-flow heat exchanger is follows.[7]

$$\varepsilon = \frac{1-\exp[-NTU\,(1-Cr)]}{1-Cr\exp[-NTU\,(1-Cr)]} \tag{6}$$

$$NTU = \frac{UA}{C_{min}} \tag{7}$$

where Cr is capacity ratio of two streams and UA is the conductance of the each element. UA is related to the convective heat transfer characteristics of two stream and conduction through the wall of the tube according to

$$UA = \frac{1}{\frac{1}{hc_{high}A_{high}} + \frac{\ln(D_{t0}/D_{ti})}{2\pi k_t L_t} + \frac{1}{\eta hc_{low} A_{low}}} \tag{8}$$

$$\eta = 1 - \frac{A_{fin}}{A_{tube}}(1-\eta_f) \tag{9}$$

where A_{high} is the inner surface of the finned tube, A_{low} is the outer surface of the finned tube, η is the efficiency of the fin and η_f is the adiabatic fin efficiency. The heat transfer characteristics of the heat exchanger is highly dependent on the local distribution of the pressure and temperature. Heat transfer coefficients of each element for high pressure gas and low pressure gas could be expressed as[7]

$$\frac{hc_{high} D_{ti}}{k} = 0.023\,Re^{0.8}Pr^{1/3}\left(1 + 3.5\frac{D_{ti}}{D_H}\right) \tag{10}$$

$$\frac{hc_{low} D_{low}}{k_{low}} = 0.26Re^{0.6}\,Pr^{1/3} \tag{11}$$

where D_H is the diameter of the helix and D_{low} is the hydraulic diameter of the passage of the low pressure returning gas as shown in Figure 3.

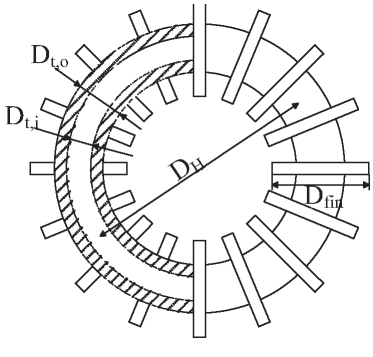

Figure 3. Cross-sectional view of a recuperative heat exchanger.

The pressure drop of the each element along the longitudinal direction could be calculated according to

$$\frac{dP_{high}}{dx} = -\left(\frac{f_{high}}{2\,D_{ti}}\rho U^2\right) - \frac{d\rho U^2}{dx} \tag{12}$$

$$\frac{dP_{low}}{dx} = \left(\frac{f_{low}}{2}\rho U^2\right) + \frac{d\rho U^2}{dx} \tag{13}$$

where U is the gas velocity of each element and x is the longitudinal direction of the heat exchanger. The friction factors of each element for high pressure gas and low pressure gas could be calculated according to[8]

$$f_{high} = \frac{0.184}{Re^{0.2}}\left(1 + 3.5\frac{D_{ti}}{D_H}\right) \tag{14}$$

$$f_{low} = (\,0.088 + 0.16\,X_L\,(X_T - 1)^{-n}\,)\,\frac{2}{Re^{0.15}} \tag{15}$$

$$n = 0.43 + \frac{1.13}{x_L} \tag{16}$$

where X_T is the non-dimensional transverse pitch and X_L is the longitudinal pitch of the finned tube. Thermodynamic properties of the gas are varied along the high pressure and low pressure passages. In the analysis, the thermodynamic properties from the REFPROP[1] were used to account the J-T cooling effects of the gas.

The geometric dimensions of the recuperative heat exchanger are listed in Table 1. The analysis was carried out for the nitrogen and argon gas with inlet pressures of 10, 20, 30, 40, 50 MPa and at 300 K.

RESULTS AND DISCUSSION

The heat exchanger effectiveness has significant effects on the liquefied yield fraction of the cryogen and the cooling capacity of the J-T refrigerator.

Figure 4 shows the variation of the effectiveness of the heat exchanger with different mass flow rates for nitrogen gas. The effectiveness decreases as the mass flow rate increases. The decrease in the effectiveness comes from the decrease of the heat exchanger NTU.

The effectiveness at 10 MPa is significantly lower than the effectiveness when the pressure is above 20 MPa. The effectiveness is almost the same when the inlet pressure is above 30 MPa.

The ideal cooling capacity of the J-T refrigerator is shown in Figure 5 as a function of the mass flow rate for nitrogen gas. The ideal cooling capacity increases as the mass flow rate through the

Table 1. Dimensions of a recuperative heat exchanger

Parameters	Value
Diameter of helix	4.070 mm
Inner diameter of tube	0.3 mm
Outer diameter of tube	0.5 mm
Pitch of tube	0.95 mm
Number of turn of tube	42
Height of fin	0.2 mm
Pitch of fin	0.132 mm
Thickness of fin	0.08 mm
Number of fin per revolution of tube	55

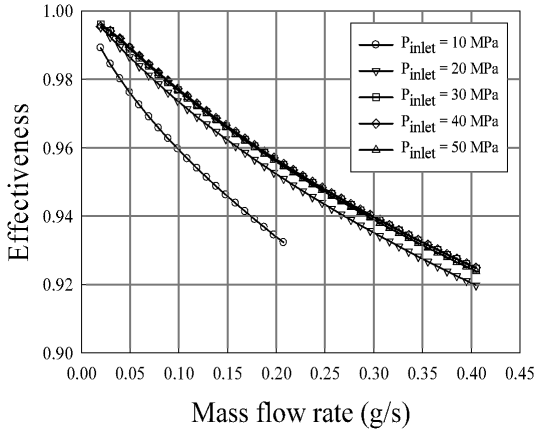

Figure 4. Variation of the effectiveness with different mass flow rates of the nitrogen gas.

heat exchanger increases. At the higher inlet pressure, the ideal cooling capacity is more linearly proportional to the mass flow rate.

There exists an optimal mass flow rate for the maximum of the ideal cooling capacity wirh the inlet pressure of 10 Mpa and 20 MPa. At the pressure of 20 MPa, the maximum of ideal cooling capacity occurs when the mass flow rate is about 3 times larger than that of the pressure of 10 MPa. At the pressure of 10 MPa and above mass flow rate of 0.2 g/s, the J-T refrigerator does not have the cooling capacity due to the small effectiveness of the heat exchanger.

The ideal cooling capacity is higher for higher pressure up to 40 MPa. The results show that the ideal cooling capacity of 50 MPa is below the 40 MPa. The thermodynamic characteristics (enthalpy) of the nitrogen gas results in the decrease of the cooling capacity.

Figure 6 shows the variation of the effectiveness of the heat exchanger with different mass flow rates of the argon gas. It is clear that the heat exchanger with the argon gas has the high effectiveness.

Figure 7 shows the variation of the ideal cooling capacity of the heat exchanger with different mass flow rates of the argon gas. There exists an optimal mass flow rate for the maximum of ideal cooling capacity at the inlet pressure of 10 MPa. At 10 MPa, the refrigerator with the argon gas has the wide operating range of the mass flow rate up to 0.43 g/s.

The refrigerator with argon gas as a cryogen has a higher ideal cooling capacity than one with nitrogen gas as a cryogen. At the higher inlet pressure, the ideal cooling capacity is more linearly proportional to the mass flow rate than that of the nitrogen.

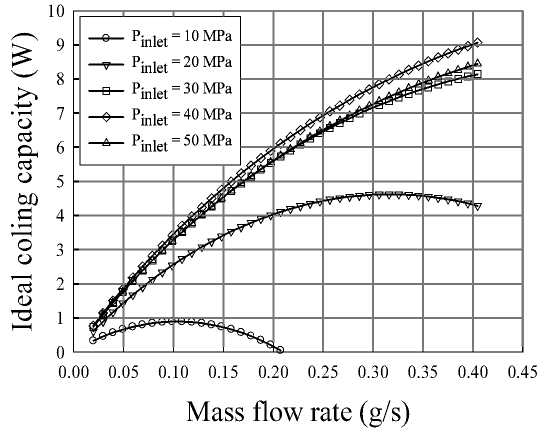

Figure 5. Variation of the ideal cooling capacity with different mass flow rates of the nitrogen gas.

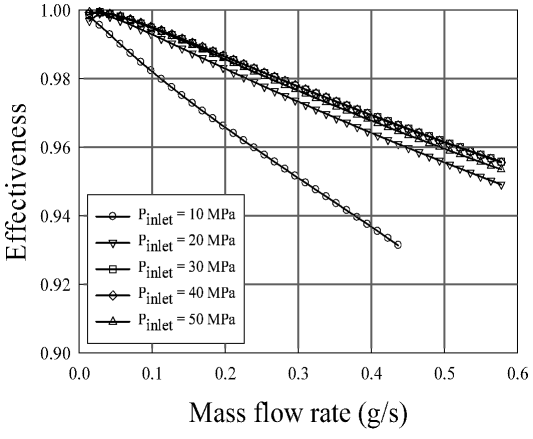

Figure 6. Variation of the effectiveness with different mass flow rates of the argon gas.

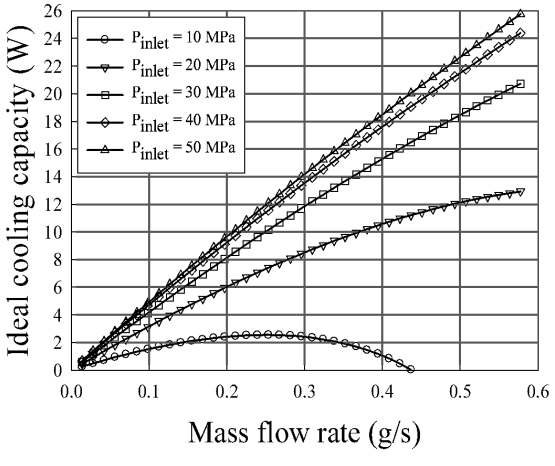

Figure 7. Variation of the ideal cooling capacity with different mass flow rates of the argon gas

Figure 8 shows the temperature and pressure profile along the longitudinal direction of the heat exchanger with the nitrogen (for the mass flow rate 0.0198 g/s (1slpm) and 0.1975 g/s (10 slpm)) at the inlet pressure of 40 MPa.

At the mass flow rate of 1 slpm, the pressure drop of the heat exchanger is negligibly small, and the temperature differences between the high pressure and low pressure gas are small due to the high effectiveness of the heat exchanger. The increases of the mass flow rate results in the increases of the pressure drop of and the relaxation of the temperature gradient.

The temperature and pressure profile of the heat exchanger with the argon (for the mass flow rate 0.0282 g/s (1slpm) and 0.2818 g/s (10 slpm)) are shown in Figure 9.

Comparison of the temperature profiles of the nitrogen and argon leads one to conclude that the argon develops a more nonlinear temperature profile along the heat exchanger than the nitrogen. It is obvious that the small pressure drop of the low pressure gas occur along the heat exchanger for the nitrogen and argon gas.

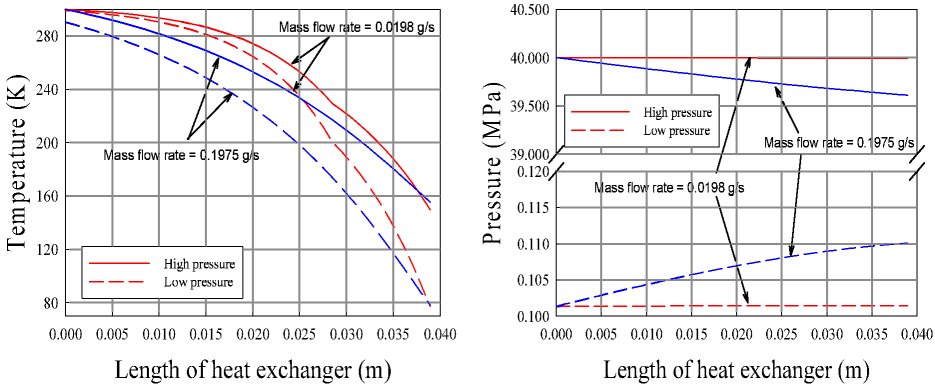

Figure 8. The temperature and pressure profile with the nitrogen at the pressure of 40 MPa.

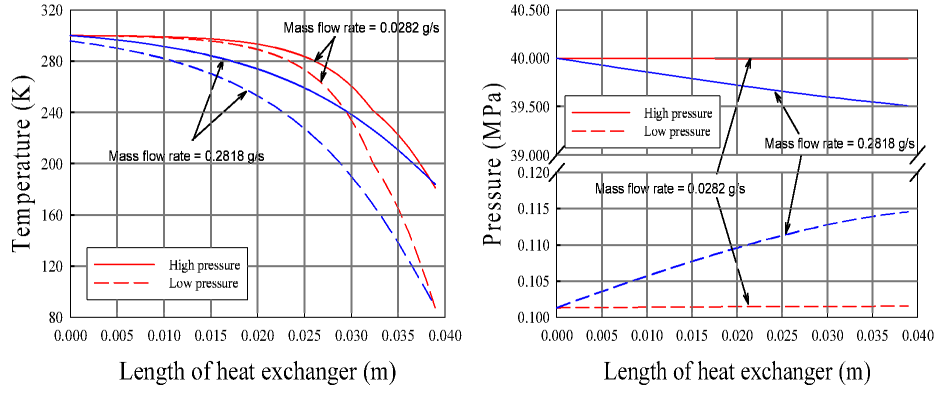

Figure 9. The temperature and pressure profile with the argon at the pressure of 40 MPa

SUMMARY

In the present study, effectiveness-NTU approach was adopted to predict the thermodynamic behaviors of the heat exchanger for the J-T refrigerator with the nitrogen and argon gas.

The results show that the effectiveness of the heat exchanger decreases as the mass flow rate increases, but the ideal cooling capacity at high pressure do not decrease. At low pressure, the refrigerator has the limited operating range in the mass flow rate.

The argon develops a more nonlinear temperature profile along the heat exchanger than nitrogen, and the small pressure drop of the low pressure gas occur along the heat exchanger for the nitrogen and argon gas.

ACKNOWLEDGMENT

This work was supported by the “Program for the leading technology in specialized research field” from Korea Institute of Machinery & Materials.

REFERENCES

1. Lemmon, E. W., McLinden, M. O., Huber, M. L., *NIST Reference Fluid Thermodynamic and Transport Properties-REFPROP*, NIST, Boulder (2002).

2. Ng, K. C., Xue, H., Wang, J. B., "Experimental and numerical study on a miniature Joule-Thomson cooler for steady-state characteristics," *Int. J. of Heat and Mass Transfer*, Vol. 45 (2002), pp. 609–618.

3. Xue, H., Ng, K.C., Wang, J.B., "Performance evaluation of the recuperative heat exchanger in a miniature Joule-Thomson cooler," *Applied Thermal Engineering*, Vol. 21 (2001), pp.1829 -1844.

4. Chien, S. B., Chen, L. T., Chou, F. C., "A study on the transient characteristics of a self-regulating Joule-Thomson cryocooler," Cryogenics, Vol. 36, Issue: 12, December 1996, pp. 979-984.

5. Chou, F. C., Pai, C. F., Chien, S. B., Chen, J. S., "Preliminary experimental and numerical study of transient characteristics for a Joule-Thomson cryocooler," Cryogenics, Vol. 35, Issue: 5, May 1995, pp. 311-316.

6. Chua, H. T., Wang, X., Teo, H. Y., "A Numerical study of the Hampson-type miniature Joule-Thomson cryocooler," *Int. J. of Heat and Mass Transfer*, vol. 49 (2006), pp. 582-593.

7. Mills, A.F., *Heat and Mass Transfer*, Richard D. Irwin, Inc.,Chicago (1995)

8. Timmerhaus, K. D., Flynn, T. M., *Cryogenic Process Engineering*, Plenum Press, New York (1989).